The first polyoxoniobate-templated silver cluster with temperature-dependent luminescent emission

Biao Wu, [a,b] *Xin-Xiong Li,** [a,c] *Shou-Tian Zheng** [a] *and Jian-Ping Xie** [b]

[a] *State Key Laboratory of Photocatalysis on Energy and Environment, College of Chemistry, Fuzhou University, Fuzhou, Fujian 350108, China.*
E-mail: lxx@fzu.edu.cn; stzheng@fzu.edu.cn
[b] *Department of Chemical and Biomolecular Engineering, National University of Singapore, 4 Engineering Drive 4, 117585, Singapore.*
E-mail: chexiej@nus.edu.sg; Tel: +65 6516 1067
[c] *Key Laboratory of Advanced Energy Materials Chemistry (Ministry of Education), Nankai University, Tianjin, 300071, China.*

This file includes:

Section S1: Experiments and Methods

1. Experimental details

$^{t}BuC\equiv CAg$ and $[(CH_3)_4N]_5[H_3Nb_6O_{19}]\cdot 20H_2O$ (TMA Nb_6) were synthesized according to the literature method and confirmed by IR spectra (Fig. S1).[1, 2] All other reagents were commercially available and were used as received without further purification. The Infrared (IR) spectrum was recorded on an Opus Vertex 70 FT-IR infrared spectrophotometer in the range of 400-4000 cm^{-1}. The Thermogravimetric analysis was performed on a Mettler Toledo TGA/SDTA 851e analyzer under a nitrogen-flow atmosphere with a heating rate of 10 °C/min in the temperature of 30-1000 °C. The Powder X-ray diffraction (PXRD) patterns was measured using a Rigaku DMAX 2500 diffractometer with Cu Kα radiation ($\lambda = 1.5418$ Å). The UV-vis absorption spectrum was collected on a PerkinElmer Lambda 35 spectrophotometer. The high-resolution electrospray ionization mass spectra (ESI-MS) was recorded on Thermo Scientific Exactive Plus mass spectrometer (German) and processed on a Bruker Data Analysis (Version 4.0) software, and the simulation was performed on a Bruker Isotope Pattern software. The Luminescence was carried out on a Hitachi F-7000 spectrometer. Elemental analyses of C/H and Ag/Nb were carried out with a Vario EL III elemental analyser and an Ultima2 inductively coupled plasma spectrometer.

2. Solvothermal Syntheses

Synthesis of $[Nb_6O_{19}@Ag_{34}(C\equiv C^{t}Bu)_{24}(CH_3COO)_2]$ (Ag_{34}): $^{t}BuC\equiv CAg$ (41.8 mg, 0.22 mmol), CF_3COOAg (23.8 mg, 0.11 mmol), TMA Nb_6 (18.1 mg, 0.011 mmol), $Ni(Ac)_2\cdot 4H_2O$ (26.8 mg, 0.11 mmol), $Na_2HPO_4\cdot 12H_2O$ (36.2 mg, 0.10 mmol) and Tris (Tris(hydroxymethyl)methyl aminomethane) (35.8 mg, 0.03 mmol) were dissolved in CH_3CN (5 mL) under stirring at room temperature for 3 min, then 2 mL DMF and 100 µL H_2O were added in order at the interval of 3 min, the mixture was stirring at room temperature for 210 min, then sealed in a bottle and kept at 65 °C for 24 h, after heating, the solution was filtrated and evaporated at room temperature in dark for five days, pale yellow block crystals were crystallized from the solution. Elemental analysis calcd (%) for $H_{222}C_{148}O_{23}Nb_6Ag_{34}$ (FW = 6594.29): Ag, 55.62; Nb, 8.45; C, 26.96; H, 3.39; N, 0. Found: Ag, 54.86; Nb, 8.91; C, 27.25; H, 3.81; N, 0. Yield: ca. 27.6 % (based on Ag).

3. Synthesis Discussion

Pale yellow block crystals of **Ag_{34}** were synthesized by the solvothermal reaction of $^{t}BuC\equiv CAg$, CF_3COOAg, TMA Nb_6, $Ni(Ac)_2\cdot 4H_2O$, $Na_2HPO_4\cdot 12H_2O$ and Tris in a ternary solvent system CH_3CN-DMF-H_2O for 24 h at 65 °C. Systematic studies reveal that $^{t}BuC\equiv CAg$ served as a common source of silver ions, while CF_3COOAg as a silver salt to depolymerize the precursor because of the insolubility of silver precursors in various solvents. We use other silver salts like PhCOOAg, CF_3SO_3Ag to replace CF_3COOAg, the consequence was similar to the above experiment. However, the yield was unsatisfactory. We also found that the suitable ternary solvent system (CH_3CN-DMF-H_2O) played a crucial role in the growth of crystals of **Ag_{34}**. The crystals were initially isolated in CH_3CN-DMF-H_2O but failed in CH_3CN-DMF, which indicated that tiny amounts of water were essential for the synthesis system. The maximum amount of water in which crystals could be isolated was 300 μL by experiment. Another factor was the Tris, we use other Trihydroxyl derivatives but failed to isolate above crystal.

4. Characterization Methods

Single-crystal structure analysis: Single-crystal X-ray diffraction data for **Ag_{34}** was collected on a Bruker APEX II diffractometer at 150 (2) K equipped with a fine focus, 2.0 kW sealed tube X-ray source (Mo Kα radiation, λ = 0.71073 Å) operating at 50 kV and 30 mA. The program SADABS was used for the absorption correction. The structures were solved by the direct method and refined on F^2 by full-matrix least-squares methods using the SHELXL-2018 program package. The contribution of disordered solvent molecules to the overall intensity data of structures were treated using the SQUEEZE method in PLATON. Crystallographic data and structure refinements for **Ag_{34}** were summarized in Table. S1. CCDC 2234637 contain supplementary crystallographic data for this paper. These data can be obtained free of charge from The Cambridge Crystallographic Data Centre via www.ccdc.cam.ac.uk/data_request/cif.

Section S2: Additional Tables

Table S1 Crystallographic data of **Ag_{34}**

Empirical formula	$C_{148}H_{222}Ag_{34}Nb_6O_{23}$
Formula weight	6594.28
Crystal system	Monoclinic
Space group	$P2_1/n$
a (Å)	20.8014(15)
b (Å)	22.7333(19)
c (Å)	21.0106(18)
α (°)	90
β (°)	94.774(2)
γ (°)	90
V (Å^3)	9901.1(14)
Z	2
$F(000)$	6276
$\rho_{calcd}(mg/m^3)$	2.212
Temperature (K)	150(2)
$\mu(mm^{-1})$	3.652
Refl. Collected	189488
Independent relf.	17457
Parameters	1001
GOF on F^2	1.064
Final R indices (I= $2\sigma(I)$)	R_1 = 0.0733, wR_2 = 0.2092
R indices (all data)	R_1 = 0.0762, wR_2 = 0.2103

$R_1 = \sum||Fo|-|Fc||/\sum|Fo|$. $wR_2 = [\sum w(F_o^2-F_c^2)^2/\sum w(F_o^2)^2]^{1/2}$; $w = 1/[\sigma^2(F_o^2) + (xP)^2 + yP]$, $P = (F_o^2 + 2F_c^2)/3$, where x = 0.0632, y = 524.4409 for **Ag_{34}**.

Table S2 The formula of the key species detected in positive-ion mode ESI-MS of **Ag_{34}** dissolved in MeOH.

Peak	Species	Exp. m/z	Sim. m/z
1A	$[Ag_{33}(Nb_6O_{19})(^tBuC\equiv C)_{22}]^{3+}$	2068.9204	2069.0239
1B	$[Ag_{34}(Nb_6O_{19})(^tBuC\equiv C)_{23}]^{3+}$	2132.2471	2131.6892
1C	$[Ag_{35}(Nb_6O_{19})(^tBuC\equiv C)_{24}]^{3+}$	2194.9043	2194.6906
1D	$[Ag_{36}(Nb_6O_{19})(^tBuC\equiv C)_{25}]^{3+}$	2258.5635	2257.6919

1E	$[Ag_{37}(Nb_6O_{19})(^tBuC\equiv C)_{26}]^{3+}$	2320.5559	2320.6933
1F	$[Ag_{31}(Nb_6O_{19})(^tBuC\equiv C)_{21}]^{2+}$	2954.9429	2954.5960
1G	$[Ag_{32}(Nb_6O_{19})(^tBuC\equiv C)_{22}]^{2+}$	3048.9385	3049.0980
1H	$[Ag_{33}(Nb_6O_{19})(^tBuC\equiv C)_{21}(CH_3COO)_2]^{2+}$	3122.3701	3121.5083
1I	$[Ag_{33}(Nb_6O_{19})(^tBuC\equiv C)_{23}]^{2+}$	3143.9211	3143.6001
1J	$\{[Ag_{33}(Nb_6O_{19})(^tBuC\equiv C)_{23}]^{2+}CH_3OH\}$	3159.3806	3159.6210
1K	$\{[Ag_{34}(Nb_6O_{19})(^tBuC\equiv C)_{24}]^{2+}CH_3OH\}$	3253.3706	3254.1230
1L	$\{[Ag_{35}(Nb_6O_{19})(^tBuC\equiv C)_{25}]^{2+}CH_3OH\}$	3348.8582	3348.6250
1M	$\{[Ag_{36}(Nb_6O_{19})(^tBuC\equiv C)26]^{2+}CH_3OH\}$	3443.3455	3443.1271
1N	$\{[Ag_{37}(Nb_6O_{19})(^tBuC\equiv C)27]^{2+}CH_3OH\}$	3537.8428	3537.6291

Section S3: Additional Figures and Characterizations

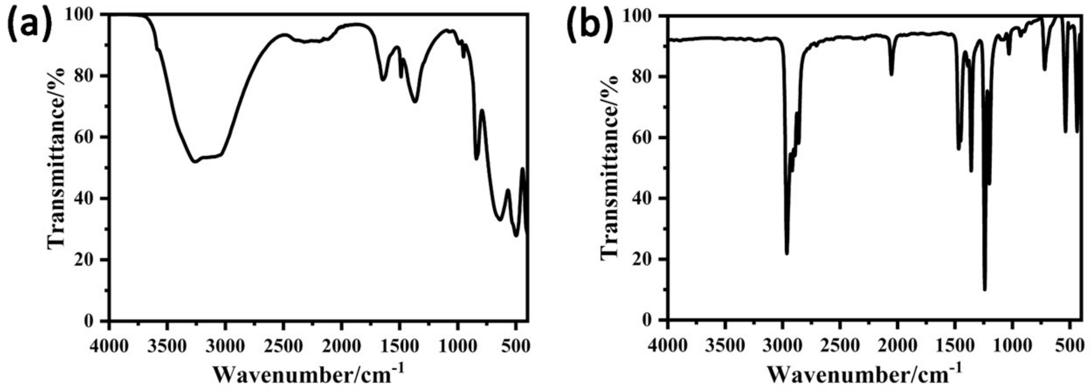

Fig. S1 (a) IR spectrum of TMA Nb_6. **(b)** IR spectrum of ${}^tBuC{\equiv}CAg$.

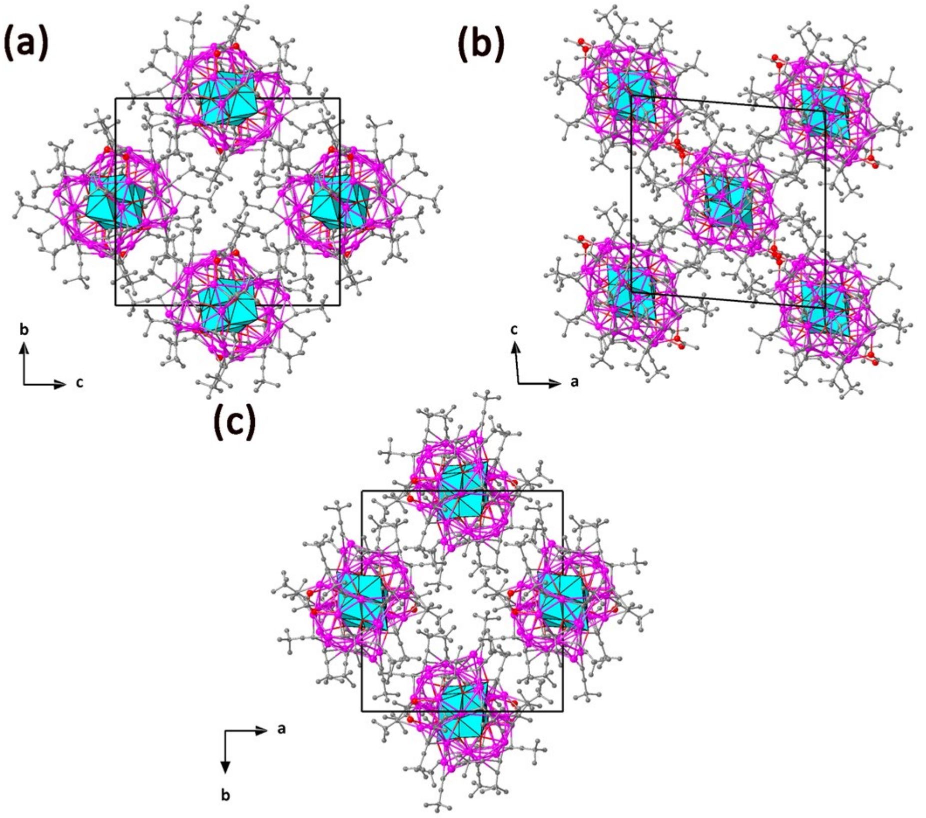

Fig. S2 The crystal packing diagrams of $\mathbf{Ag_{34}}$ in one unit cell viewed along *a* **(a)**, *b* **(b)** and *c* **(c)** axis. Color code: magenta, Ag; red, O; gray, C; cyan, Nb. The cyan polyhedra represent $[Nb_6O_{19}]^{8-}$ template.

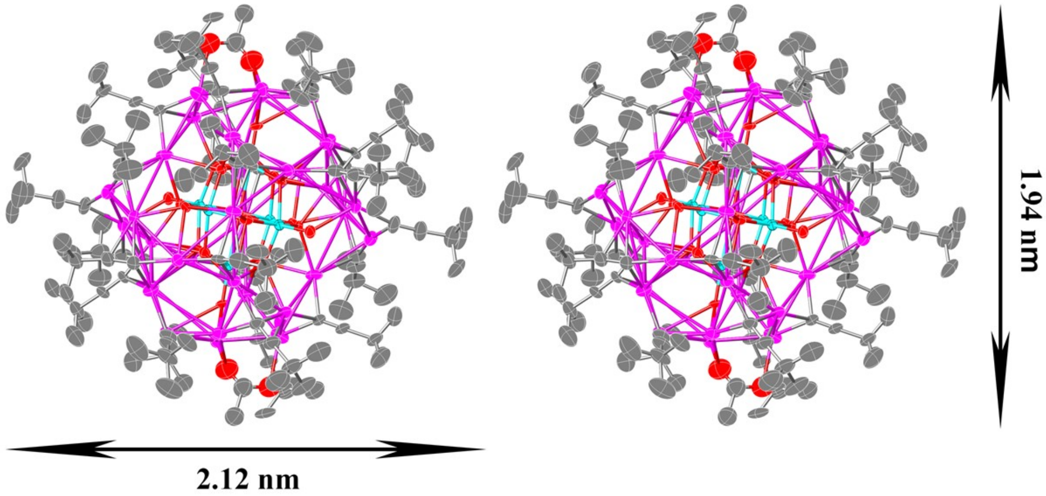

Fig. S3 The diameters of **Ag_{34}** with all H atoms omitted for clarity. Color code: magenta, Ag; red, O; gray, C; cyan, Nb.

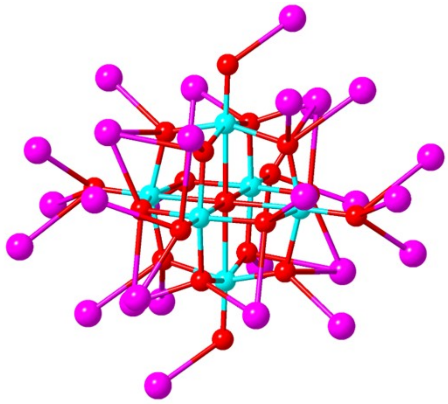

Fig. S4 The coordination modes of $[Nb_6O_{19}]^{8-}$ anion towards 28 silver atoms. Color code: magenta, Ag; red, O; gray, C; cyan, Nb.

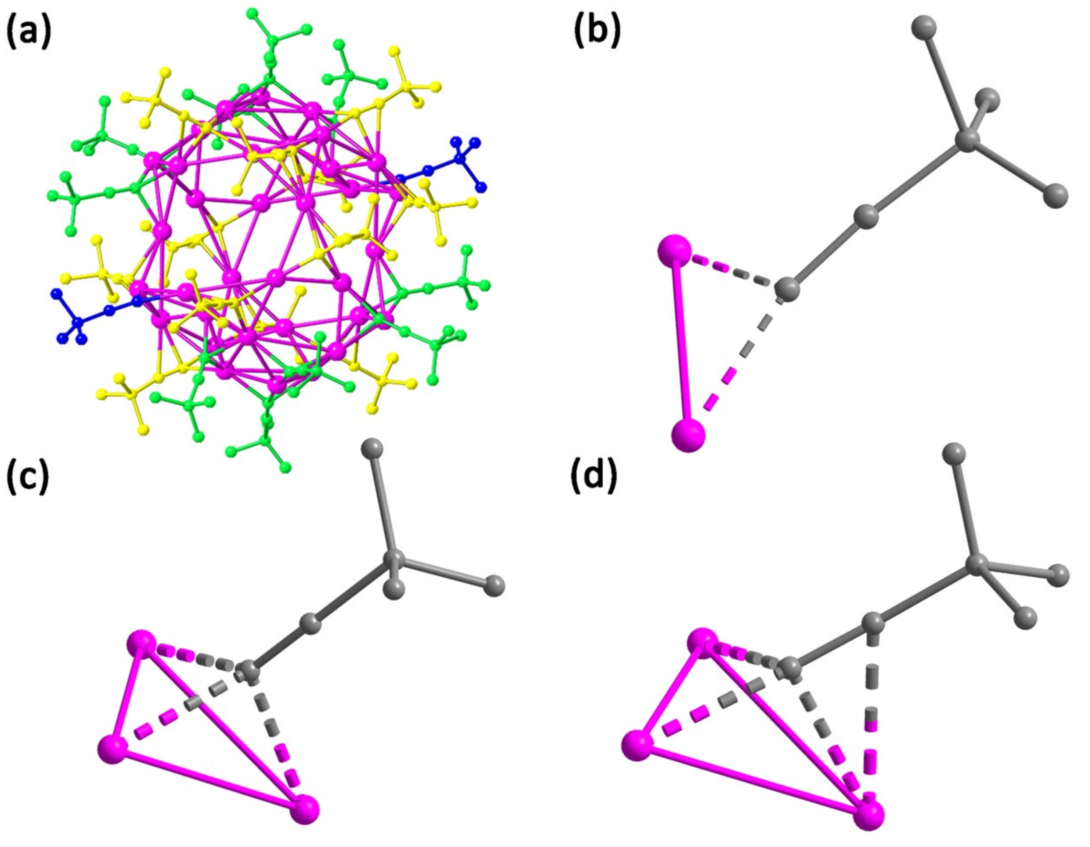

Fig. S5 (a) The coordination modes of 22 ^{t}BuC≡C ligands towards silver atoms in **Ag$_{34}$**. **(b)** Blue: 2 in μ_2-$\eta^1\eta^1$; **(c)** Green: 10 in μ_3-$\eta^1\eta^1\eta^1$; **(d)** Yellow: 12 in μ_3-$\eta^1\eta^1\eta^2$.

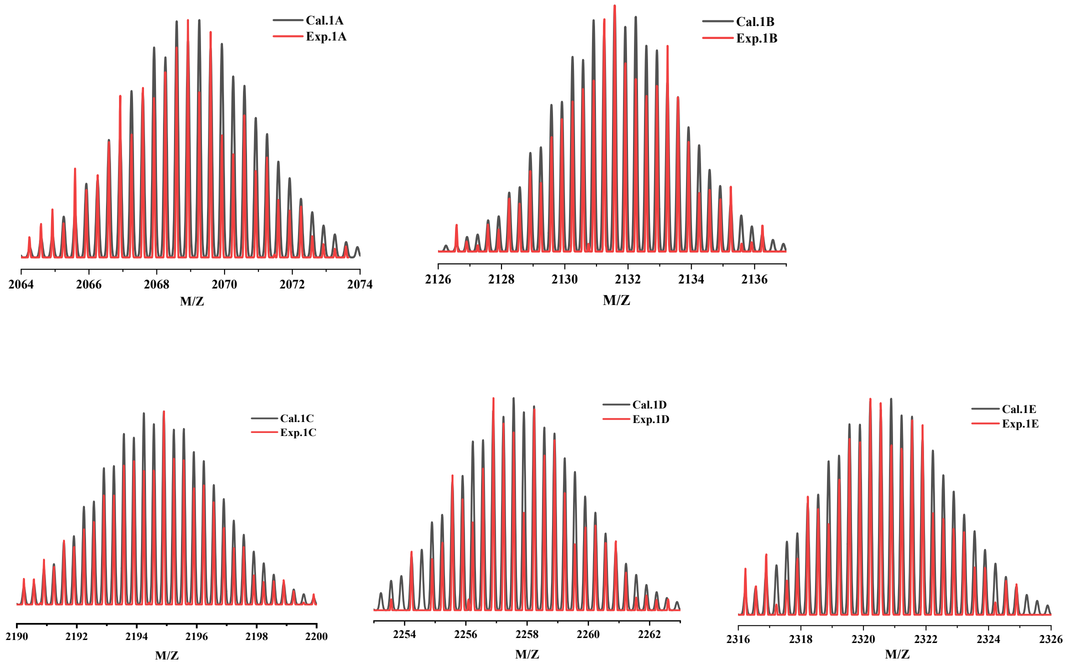

Fig. S6 The full ESI-MS spectra with the calculated (blackline) and experimental (redline) isotopic patterns for species 1A - 1E. Note: M = [Nb_6O_{19}@Ag_{34}(^{t}BuC≡C)$_{24}$(CH_3COO)$_2$].

1A = 2069.0239 : [M - $2CH_3COO$ - $2{}^{t}BuC\equiv C$ - Ag]$^{3+}$

1B = 2131.6892 : [M - $2CH_3COO$ - $1{}^{t}BuC\equiv C$]$^{3+}$

1C = 2194.6906 : [M - $2CH_3COO$ + Ag]$^{3+}$

1D = 2257.6919 : [M - $2CH_3COO$ + $1{}^{t}BuC\equiv C$ + 2Ag]$^{3+}$

1E = 2320.6933 : [M - $2CH_3COO$ + $2{}^{t}BuC\equiv C$ + 3Ag]$^{3+}$

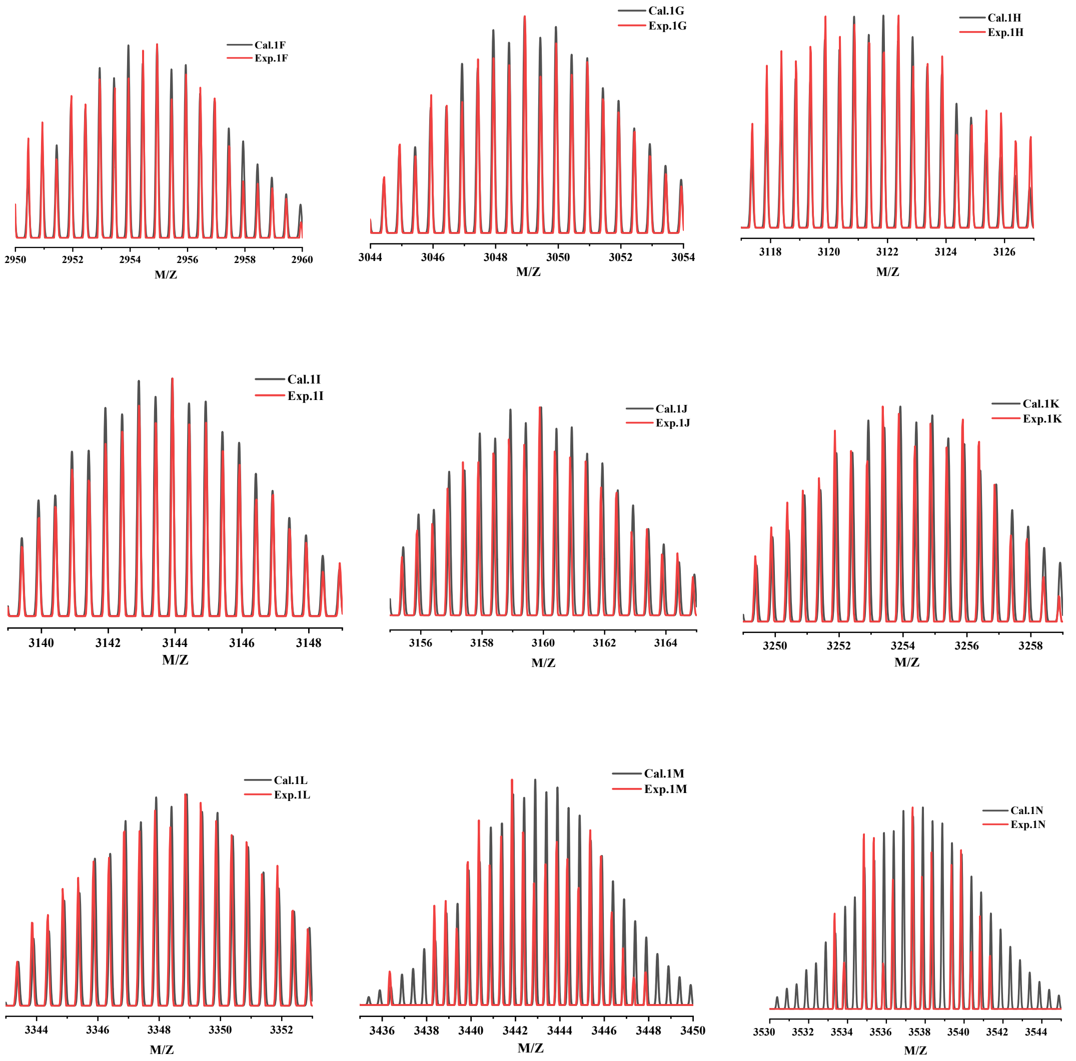

Fig. S7 The full ESI-MS spectra with the calculated (blackline) and experimental (redline) isotopic patterns for species 1F-1N. Note: M = [$Nb_6O_{19}@Ag_{34}({}^{t}BuC\equiv C)_{24}(CH_3COO)_2$].

1F = 2954.5960 : [M - $2CH_3COO$ - $3{}^{t}BuC\equiv C$ - 3Ag]$^{2+}$

1G = 3049.0980: [M - $2CH_3COO$ - $2{}^{t}BuC\equiv C$ - 2Ag]$^{2+}$

1H = 3121.5083: [M - $3{}^{t}BuC\equiv C$ - Ag]$^{2+}$

1I = 3143.6001: [M - $2CH_3COO$ - ${}^{t}BuC\equiv C$ - Ag]$^{2+}$

1J = 3159.6210: [M - $2CH_3COO$ - ${}^{t}BuC\equiv C$ - Ag + CH_3OH]$^{2+}$

1K = 3254.1230 : [M - $2CH_3COO$ + CH_3OH]$^{2+}$

1L = 3348.6250: [M - $2CH_3COO$ + ${}^{t}BuC\equiv C$ + Ag + CH_3OH]$^{2+}$

1M = 3443.1271: [M - $2CH_3COO$ + $2{}^{t}BuC\equiv C$ + 2Ag + CH_3OH]$^{2+}$

1N = 3537.6291: $[M - 2CH_3COO + 3^tBuC{\equiv}C + 3Ag + CH_3OH]^{2+}$

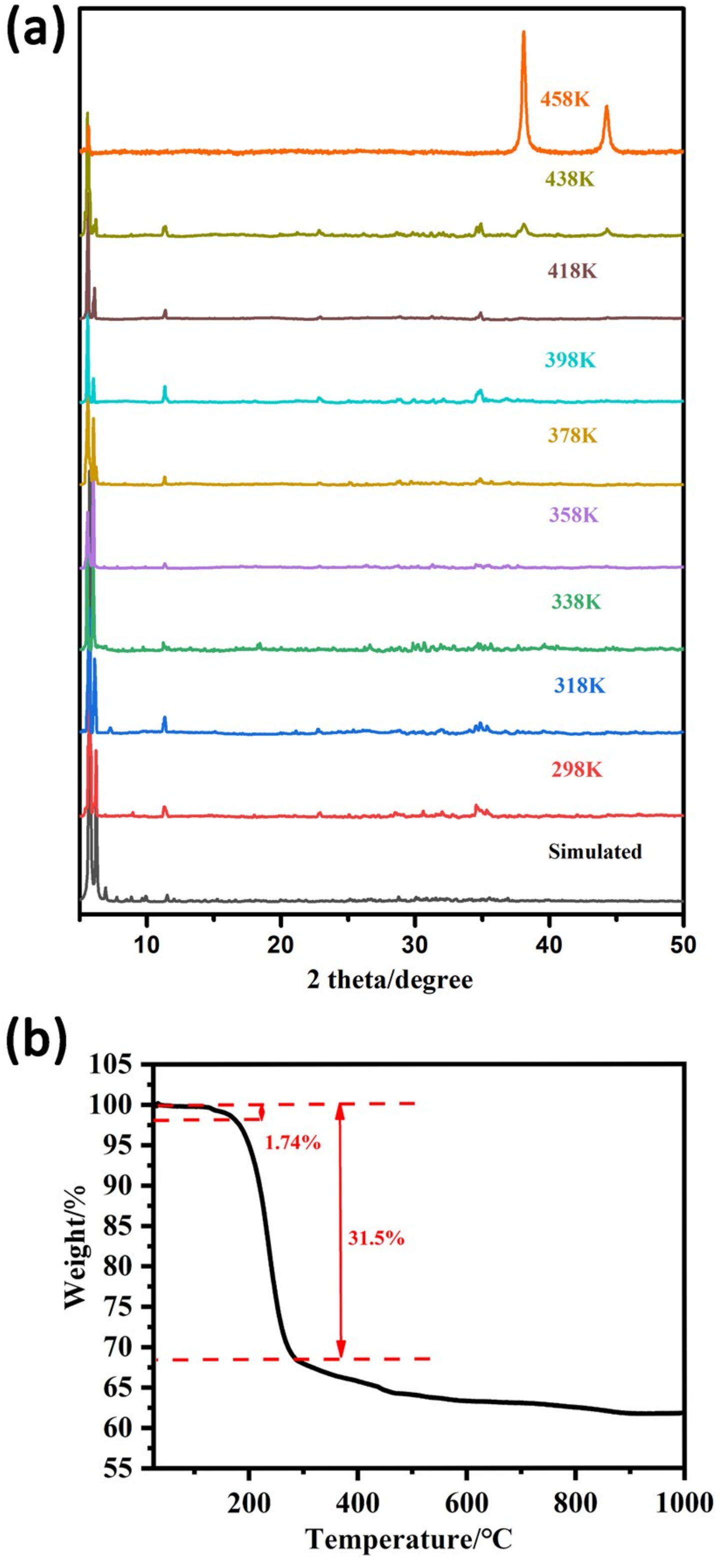

Fig. S8 The variable temperature PXRD patterns **(a)** and TGA curves **(b)** of **Ag$_{34}$** (heating rate 10℃/ min).

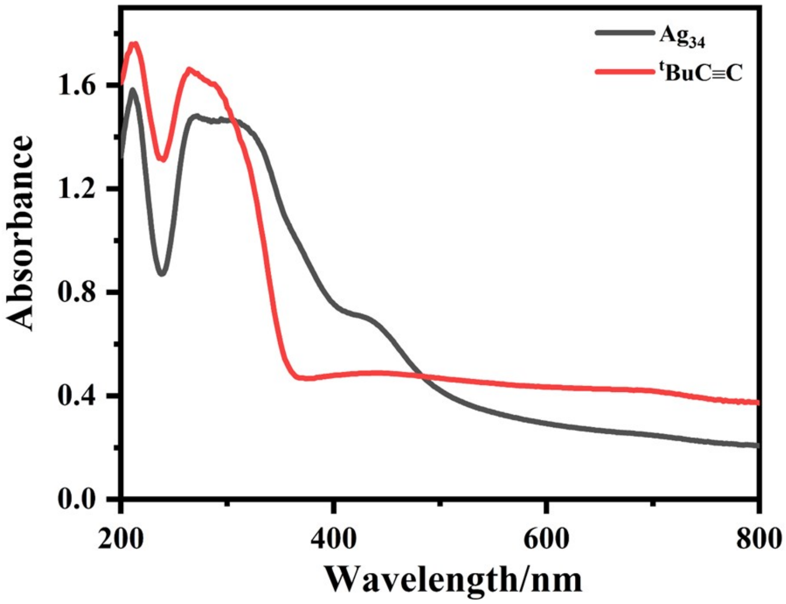

Fig. S9 Solid-state UV absorption spectrum of **Ag_{34}** and ^{t}BuC≡CAg.

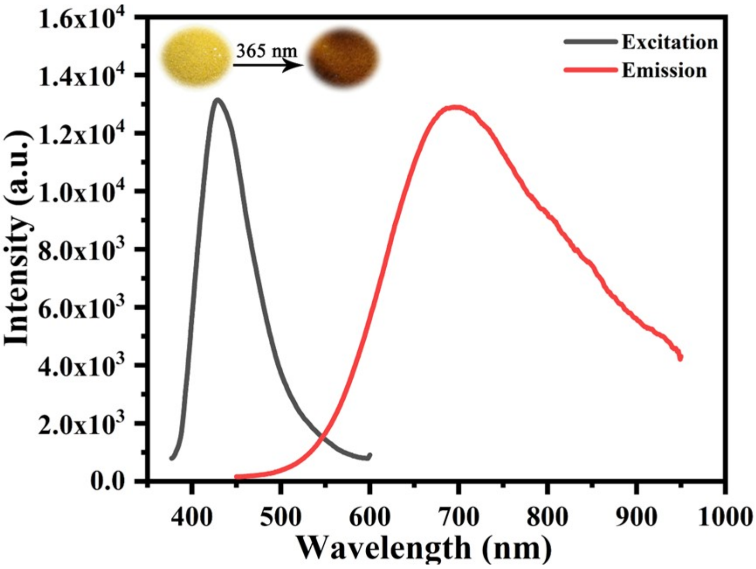

Fig. S10 Excitation and Emission spectra of **Ag_{34}** in solid state at 293 K. The inset in the top left corner shows photographs of a solid-state sample of **Ag_{34}** when excited using a hand-held UV lamp (365 nm) at room temperature.

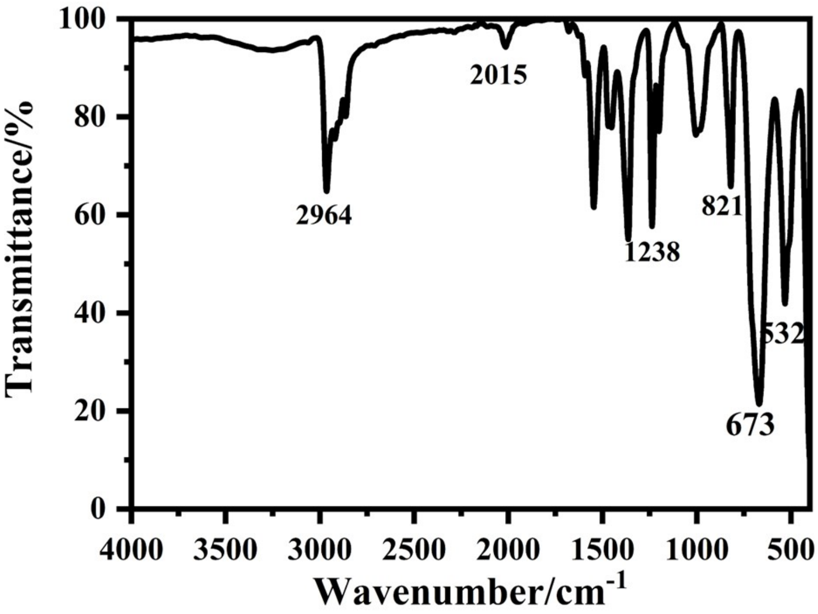

Fig S11 IR spectrum of **Ag_{34}**. The IR spectrum shows broad bands at approximately 2964, 2015, 1238, 821, 673 and 532 cm^{-1}, which were assigned to the stretching frequencies of the C−H bond of the methyl group, the C≡C bond of the alkynyl group, the C−O bonds of the acetate, and the Nb-O_t, Nb-O_b-Nb bonds of the niobium, respectively.

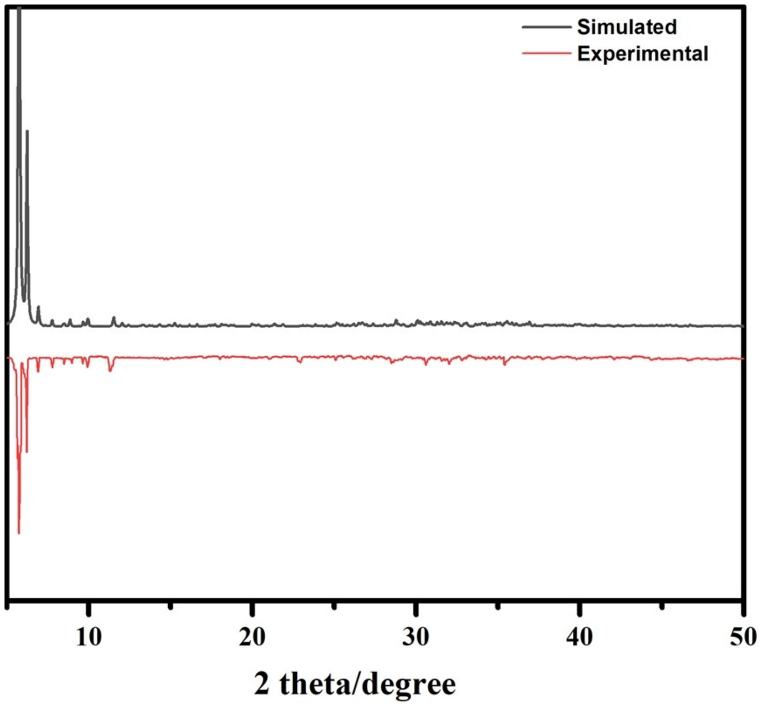

Fig S12 Experimental and simulated PXRD patterns of **Ag_{34}**.

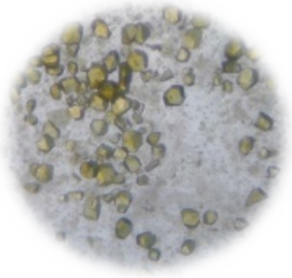

Fig. S13 The photograph of crystals of **Ag_{34}** taken under the microscope by digital camera.

Section S4: References

1. Z.-G. Jiang, K. Shi, Y.-M. Lin and Q.-M. Wang, *Chem. Commun.*, 2014, **50**, 2353-2355.
2. L. B. Fullmer, R. H. Mansergh, L. N. Zakharov, D. A. Keszler and M. Nyman, *Cryst. Growth. Des.*, 2015, **15**, 3885-3892.